Measurement of molecular polarizability anisotropy via alignment-induced spatial focusing and defocusing

Hao Li, Wenxue Li,* Yahui Feng, Jia Liu, Haifeng Pan, and Heping Zeng†
State Key Laboratory of Precision Spectroscopy, East China Normal University, Shanghai 200062, China
(Received 30 November 2011; published 29 May 2012)

We demonstrate that the polarizability anisotropy of the acetylene molecule could be experimentally determined by molecular alignment-induced spatial focusing and defocusing effects under femtosecond impulsive excitation. The molecular alignment signals of oxygen and acetylene were measured under identical experimental conditions and the polarizability anisotropy of acetylene was quantitatively determined with oxygen as the reference molecule. Meanwhile, the Kerr coefficients of oxygen and acetylene were estimated. This intuitive and simple method is also applicable to other molecules.

DOI: 10.1103/PhysRevA.85.052515 PACS number(s): 33.15.Kr, 42.65.Jx, 33.80.−b, 37.10.Vz

I. INTRODUCTION

Molecular polarizability anisotropy is one of the most intrinsic parameters of molecules that greatly affects various kinds of properties of molecules and reveals some detailed information about their electronic structures [1]. It could be theoretically calculated for some simple molecules by establishing a proper model [2] and experimentally measured via optical Rayleigh depolarization ratio [3], molecular beam magnetic resonance [4], Stark effect via microwave spectroscopy [5], or Coulomb explosion experiment [6]. Furthermore, molecules with a polarizability anisotropy experience angular-dependent impulsive interactions with intense linearly polarized laser pulses, which force them to align or orient along the polarization of the exciting pulses. This has sparked intriguing applications in high-order harmonic generation control [7,8], full-dimensional molecular manipulation [9], and molecular-orbital reconstruction [10]. Molecular alignment was also demonstrated to induce spatiotemporal phase modulation [11], which provides additional degrees of freedom to control ultrashort pulse compression [12], central wavelength tuning of few-cycle ultrashort pulses [13], spatial focusing and defocusing and regularization [14], as well as filament propagation and interactions [15]. Interestingly, different molecular structures or properties exhibit different alignment characteristics and these differences exactly reveal the rotational dynamics after the impulsive preexcitation, facilitating some methods to retrieve polarizability anisotropies and other intrinsic molecular parameters requisite for molecular chemistry and physics.

In this paper, we demonstrate a direct retrieval of molecular polarizability anisotropy and optical nonlinearity by a simple and robust temporal-scan (τ-scan) technique with a weak probe pulse delayed around the field-free revivals of the preexcited rotational wave packets. The spatial focusing or defocusing was sensitively dependent upon the spatiotemporal cross-phase-modulation induced by alignment and accordingly, a continuous τ scan from the parallel to perpendicular molecular revivals made the weak probe pulse change from focusing to defocusing. This is quite similar to the spatial-scan (z-scan) technique widely used to characterize third-order optical nonlinearity [16]. Here, the z scan of nonlinear optical samples nearby the light focus is replaced by the τ scan of the probe pulse around the molecular revivals, and the τ-scan technique typically exhibits an improved sensitivity applicable to various gaseous molecules. The alignment signals of oxygen molecule (O_2) and acetylene molecule (C_2H_2) were measured under identical experimental conditions. Taking O_2 as the reference molecule, whose polarizability anisotropy is available, we quantitatively retrieve the polarizability anisotropy of C_2H_2 by comparing their molecular alignment signals. Moreover, the optical nonlinearity of gaseous molecules could also be derived from the τ-scan technique through a careful analysis of the combined spatial focusing arising from molecular alignment and optical Kerr effect.

In general, the aligned molecules could be described by the angle θ between the molecular axis and the polarization of the exciting field. The molecular alignment degree should be averaged over all thermally populated rotational states of the involved molecules, yielding a statistic metric $\langle\langle\cos^2\theta\rangle\rangle$, which is a complex function of the ambient temperature T, spatiotemporal characteristics of the exciting field ε, and the molecular polarizability anisotropy $\Delta\alpha = \alpha_{||} - \alpha_{\perp}$ ($\alpha_{||}$ and $\alpha_{\perp}$ are the components parallel and perpendicular to the molecular axis), i.e., $\langle\langle\cos^2\theta(\tau)\rangle\rangle \approx f(\tau, T, \varepsilon, \Delta\alpha)$ [17]. The molecular alignment induced an instantaneous modulation of the refractive index as $\delta n = 2\pi(\rho_0\Delta\alpha/n_0)(\langle\langle\cos^2\theta\rangle\rangle - 1/3)$ [15], where ρ_0 and n_0 denote the molecular number density and linear refractive index of the initially randomly aligned molecules. Due to the Gaussian spatial intensity distribution of the exciting pulse, the refractive-index modulation δn of the central part was essentially different from that of the peripheral part and thus there existed a spatial refractive index gradient. Such a refractive index gradient acted as a convex or concave lens, leading to focusing or defocusing effects, respectively. As the probe pulse was delayed around alignment revivals, its spatial intensity distribution was correspondingly modulated.

This paper is organized as follows. After this brief introduction, we give a detailed description of the experimental setup and theoretical basis of the τ-scan measurement in Sec. II. The experimental results are presented in Sec. III together with some discussions on the τ-scan measurement sensitivity and its applicability to various gaseous molecules. A technique

*wxli@phy.ecnu.edu.cn
†hpzeng@phy.ecnu.edu.cn

for quantitative retrieval of molecular polarizability anisotropy is developed with O_2 as the reference molecule, and a careful analysis of the τ-scan measurement of optical nonlinearity of gaseous molecules is also presented in this section. A brief conclusion is given in Sec. IV.

II. EXPERIMENTAL SETUP AND THEORETICAL BASIS

As schematically shown in Fig. 1(a), our experiments were carried out with an amplified Ti:sapphire laser system (800 nm, 1 kHz). The pulse was split into two parts: One was used to align the molecules (aligning pulse), the other was sent to a β-barium borate crystal (type-I, 29.2°-cut, 100-μm thick) to generate the second harmonic probe pulse. The polarization of the aligning pulse was set to be parallel to that of the probe pulse by an 800-nm half-wave plate. The aligning and probe pulses were respectively focused by two separated convex lenses of $f = 80$ and 60 cm and collinearly combined with a dichroic mirror. The convex lenses were properly positioned to have their foci spatially overlapped in the interaction region. The aligning and probe pulses were measured to be ~71.0 and ~0.4 μJ after the combining glass plate, respectively. The peak intensity of the aligning pulse (~0.5×10^{13} W/cm^2) was intense enough to align the molecules, but its peak power (~1.3 GW) was far away from the critical power for filamentation in air (~4.5 GW) [18], so that there almost existed no multi-photon-ionization-induced plasma to exert any possible detrimental plasma influence on the field-free molecular alignment. The temporal duration of the aligning pulse was measured to be ~60 fs FWHM. The gas cell placed around the laser foci was filled with 1-atm gaseous molecules at a constant temperature ~23.1 °C. In order to remove the influence of the 800-nm aligning pulse, the 400-nm probe pulses were extracted after the gas cell with four 400-nm high-reflection mirrors. After an iris, the center part of the probe pulse was focused into a detector with a lens ($f = 10$ cm) for alignment signal measurement. The iris diameter ($D \approx 3$ mm) was smaller than that of the probe beam (~10 mm) and only its central part got through the aperture (detection area). As showed in Fig. 1(b), the spatial distribution

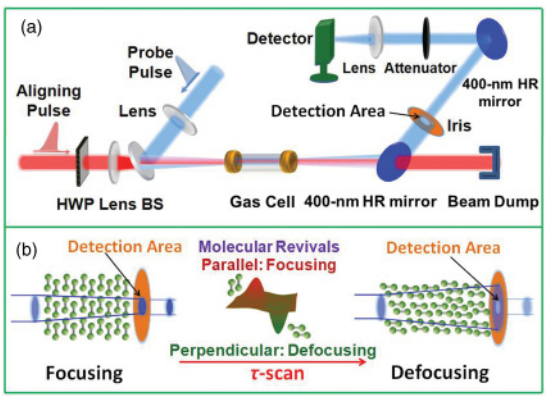

FIG. 1. (Color online) (a) The experimental setup. (HWP) 800-nm half-wave plate; (400-nm HR mirror) 400-nm high-reflection mirror; (BS) beam splitter. (b) The schematic diagram of τ-scan technique and the spatial distribution modulations of focusing and defocusing effects.

of the probe beam was modulated by spatial focusing and defocusing and the modulation at different delays could be revealed by measuring the probe intensity signals after the aperture, which is equivalent to a lens with a focal length [19]

$$f_m \propto n_0 w_0^2 / \{4d[\langle\langle \cos^2\theta(\tau)\rangle\rangle_{r=0} - 1/3]\}, \tag{1}$$

where n_0, w_0, and d denote the linear refractive index, pump beam waist, and effective interaction length, respectively. As the focusing and defocusing effects induced by alignment revivals occur, the pulse energy within the detection area could be calculated to be [20]

$$\begin{aligned} S_D(\tau) &= 2\int_0^{D/2} I(r,\tau)dr = \frac{S_{D0}}{1 \mp \eta[\langle\langle \cos^2\theta(\tau)\rangle\rangle_{r=0} - 1/3]} \\ &\approx S_{D_0}\{1 \pm \eta[\langle\langle \cos^2\theta(\tau)\rangle\rangle_{r=0} - 1/3]\}, \end{aligned} \tag{2}$$

where S_{D_0} is the measured signal without molecular alignment (background) and $\eta \approx 4dZ_0^2\rho_0\Delta\alpha/[(Z_0^2/L + L)w_0^2]$ is a small parameter, with the distance L between iris and interaction point ($L \approx 1$ m) being much larger than the Rayleigh length Z_0 ($Z_0 \approx 2$ cm) [20]. In general, a homodyne detection, such as the weak field polarization technique [21] or cross-defocusing measurement [20], could only obtain a signal proportional to $(\delta n)^2$ or $(\langle\langle \cos^2\theta\rangle\rangle - 1/3)^2$, from which parallel and perpendicular alignment cannot be distinguished. Equation (2) shows that the τ-scan measurement here is equivalent to heterodyne detection [22] rather than homodyne detection, yielding a net signal $\Delta S(\tau) = S_D(\tau) - S_{D_0}$ proportional to δn or $\langle\langle \cos^2\theta(\tau)\rangle\rangle - 1/3$.

When an anisotropic linear molecule is subjected to an intense linearly polarized laser field, the laser-molecular interaction is closely related to the molecular polarizability anisotropy $\Delta\alpha$ as [17]

$$H_{\text{eff}}(\tau) = B\mathbf{J}^2 - 1/2\varepsilon^2(\tau)[\Delta\alpha\cos^2\theta + \alpha_\perp], \tag{3}$$

where B, $\mathbf{J}$, and ε denote the rotational constant, rotational angular momentum operator, and the applied aligning field, respectively. By assuming the initial rotational wave function as the superposition of a series of field-free rotor eigenfunctions

$$|\psi(\tau)\rangle = \sum_{JM} d_{JM}(\tau)|JM\rangle, \tag{4}$$

we solved the Schrödinger equation and calculated the evolution of the rotational wave function and the averaged value $\langle\langle \cos^2\theta(\tau)\rangle\rangle$. More specifically, for each initial rotational state

$$|\psi(\tau = 0)\rangle = |J_0M_0\rangle, \tag{5}$$

we determined its evolution with the fourth-order Runge-Kutta method by the Schrödinger equation

$$i\hbar\partial\psi(\tau)/\partial\tau = H_{\text{eff}}(\tau)\psi(\tau). \tag{6}$$

Then we calculated its contribution $\langle\cos^2\theta(\tau)\rangle_{J_0M_0}$ by [14]

$$\langle\cos^2\theta(\tau)\rangle_{J_0M_0} = \sum_{JM,J'M'} d^*_{JM}(\tau)d_{J'M'}(\tau)\langle JM|\cos^2\theta|J'M'\rangle. \tag{7}$$

Actually, there are only three kinds of nonvanishing matrix elements in Eq. (7): $\langle JM|\cos^2\theta|JM\rangle$, $\langle JM|\cos^2\theta|J+2,M\rangle$, and $\langle JM|\cos^2\theta|J-2,M\rangle$ [23]. As the temperature-dependent thermal population of the initial rotational states is Boltzmann distribution, the total contribution of all rotational states should be

$$f(\tau,T,I,\Delta\alpha) = \langle\langle\cos^2\theta(\tau)\rangle\rangle = \frac{\sum_{JM} g_{J_0}\exp\left(-E^{\rm rot}_{J_0}/kT\right)\langle\cos^2\theta(\tau)\rangle_{J_0M_0}}{\sum_J g_{J_0}(2J_0+1)\exp\left(-E^{\rm rot}_{J_0}/kT\right)}, \quad (8)$$

where $E^{\rm rot}_J$ and g_J denote the eigenvalue and weight factor of the rotational state J. Due to the differences in nuclear spin statistical properties, the distribution of the rotational quantum number J of various molecules may vary from one to another. The ratios between odd J and even J are 1 : 0 and 3 : 1 for oxygen and acetylene, respectively. In order to seek an accurate result, the contributions of states J up to 35 were calculated. Numerical simulations indicate that the metric $\langle\langle\cos^2\theta\rangle\rangle$ is sensitively dependent on $\Delta\alpha$ while insensitively influenced by the ambient temperature variation, which guarantees the τ-scan measurement accuracy without strict temperature control.

III. RESULTS AND DISCUSSIONS

Figure 2 shows the measured and calculated alignment signals of O_2 and C_2H_2 and the insets display the three-dimensional dynamic rotational wave packets of molecular revivals. The measured signals could be well reproduced by numeric simulations with parameters faithfully chosen according to the experimental conditions: gas temperature $T = 23.1\,^\circ$C, the peak intensity of the aligning field $I = 0.5 \times 10^{13}$ W/cm^2, and its FWHM duration $\tau = 60$ fs. The robustness of the τ-scan measurement greatly benefits from the stable characteristics of field-free molecular alignment, which are insensitive to the fluctuations of ambient temperature, exciting intensity, and the mechanical vibration of experimental setup. The features of stability even enable the aligned molecules to function as transient frequency-resolved optical gating (FROG) for ultrashort laser pulse measurement [24,25]. With the available polarizability anisotropy of $\Delta\alpha_{O_2} = 1.15$ Å^3 [26], as shown in Fig. 2(a), the theoretically calculated O_2 revivals were well fitted with the measured ones. Taking O_2 as the reference, τ-scan measurements could be readily implemented to determine the polarizability anisotropies of other molecules. For instance, by comparing the measured alignment signals of O_2 and C_2H_2 with Eq. (2), the polarizability anisotropy of acetylene $\Delta\alpha_{C_2H_2}$ could be retrieved by

$$\frac{\Delta S_{O_2}(\tau)}{\Delta S_{C_2H_2}(\tau')} = \frac{\rho_{O_2}\Delta\alpha_{O_2}[\langle\langle\cos^2\theta(\tau)\rangle\rangle_{O_2} - 1/3]}{\rho_{C_2H_2}\Delta\alpha_{C_2H_2}[\langle\langle\cos^2\theta(\tau')\rangle\rangle_{C_2H_2} - 1/3]} = \frac{\rho_{O_2}\Delta\alpha_{O_2}[f(\tau,T,I,\Delta\alpha_{O_2}) - 1/3]}{\rho_{C_2H_2}\Delta\alpha_{C_2H_2}[f(\tau',T,I,\Delta\alpha_{C_2H_2}) - 1/3]}, \quad (9)$$

where $\Delta S_{O_2}(\tau)$ and $\Delta S_{C_2H_2}(\tau')$ denote the measured net probe signals of O_2 and C_2H_2, respectively. Obviously, $\Delta\alpha_{C_2H_2}$ was just the solution of Eq. (9), while $\langle\langle\cos^2\theta(\tau')\rangle\rangle_{C_2H_2}$ was actually the function of $\Delta\alpha_{C_2H_2}$ and could be denoted as $f(\tau',T,I,\Delta\alpha_{C_2H_2})$. So Eq. (9) could be transformed into

$$\Delta\alpha_{C_2H_2}[f(\tau',T,I,\Delta\alpha_{C_2H_2}) - 1/3] = \frac{\Delta S_{C_2H_2}(\tau')}{\Delta S_{O_2}(\tau)}\frac{\rho_{O_2}}{\rho C_2H_2}\Delta\alpha_{O_2}[f(\tau,T,I,\Delta\alpha_{O_2}) - 1/3]. \quad (10)$$

On the left side of Eq. (10), there must be one unique $\Delta\alpha_{C_2H_2}$ which fulfills Eq. (10). Therefore, with the measured $\Delta S_{C_2H_2}(\tau')/\Delta S_{O_2}(\tau)$, we can quantitatively seek the unknown $\Delta\alpha_{C_2H_2}$. Taking the delays C and c in Fig. 2 for instance, we chose a properly estimated value $\Delta\alpha_{C_2H_2}$ (for example, 1.50 Å^3) and calculated $f(\tau_c,T,I,\Delta\alpha_{C_2H_2})$. By comparing the magnitudes of both sides, we could judge whether the estimated $\Delta\alpha_{C_2H_2}$ should be revised to be larger or smaller to fulfill Eq. (10). The value of $\Delta\alpha_{C_2H_2}$ was gradually revised, with $f(\tau_c,T,I,\Delta\alpha_{C_2H_2})$ continuing to update with new $\Delta\alpha_{C_2H_2}$, until Eq. (10) became true and thus the unknown $\Delta\alpha_{C_2H_2}$ was found. For delays C and c, $\Delta\alpha_{C_2H_2}$ was calculated to be 1.73 Å^3 while delays D and d yield a value of 1.72 Å^3. However, the measured alignment signals suffered an exponential decay due to a collision relaxation process so that Eq. (9) should be corrected with a decay factor:

$$\frac{\Delta S_{O_2}(\tau)}{\Delta S_{C_2H_2}(\tau')} = \frac{e^{-\lambda_{O_2}\tau}}{e^{-\lambda_{C_2H_2}\tau'}}\frac{\rho_{O_2}\Delta\alpha_{O_2}[f(\tau,T,I,\Delta\alpha_{O_2}) - 1/3]}{\rho_{C_2H_2}\Delta\alpha_{C_2H_2}[f(\tau',T,I,\Delta\alpha_{C_2H_2}) - 1/3]}, \quad (11)$$

where the decay coefficients λ_{O_2} and $\lambda_{C_2H_2}$ could be calculated by the measured signals. Taking delays B and E in Fig. 2(a) for example, λ_{O_2} can be obtained by $\Delta S(\tau_E)/\Delta S(\tau_B) = e^{-\lambda(\tau_E-\tau_B)}$. The average values of λ_{O_2} and $\lambda_{C_2H_2}$ were ~0.044 and ~0.041 ps^{-1} and the decay factors were implemented for the

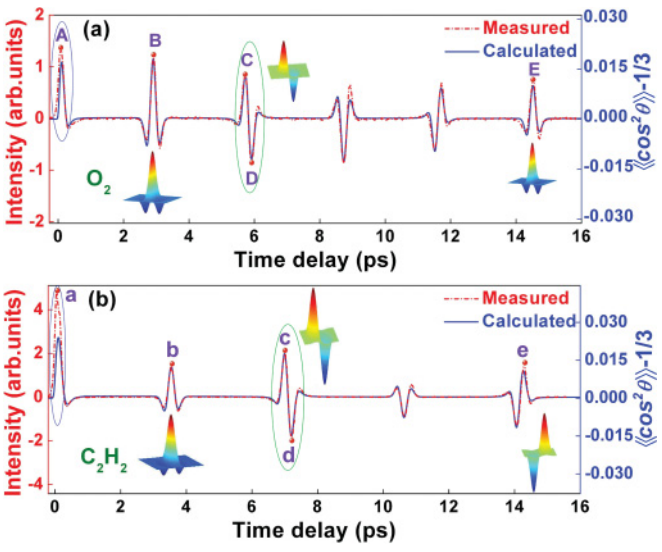

FIG. 2. (Color online) (a), (b) Measured (red dash-dot line) and calculated (blue solid line) molecular alignment signals of O_2 and C_2H_2, respectively. The measured field-free alignment signals in delays C (c) and D (d) were used to retrieve the polarizability anisotropy of acetylene while the signals around the zero-time delay in delays **A** and **a** were used to estimate the Kerr coefficients of oxygen and acetylene, respectively. The insets show the dynamic rotational wave packets of molecules.

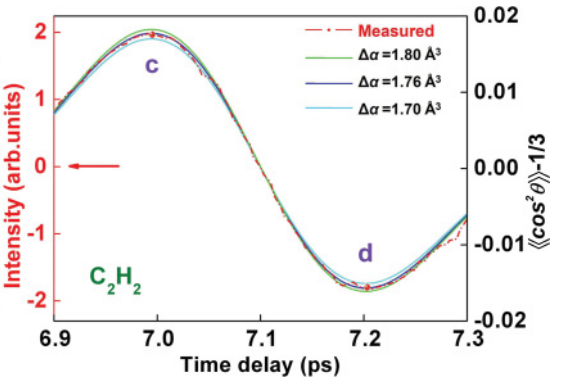

FIG. 3. (Color online) The measured signals (red dash-dot line) and calculated signals of C_2H_2 around delays c and d with $\Delta\alpha_{C_2H_2} = 1.80$ Å^3 (green solid line), 1.76 Å^3 (blue solid line), 1.70 Å^3 (cyan solidline).

calculated signals in Fig. 2. After such a correction, the results became $\Delta\alpha_{C_2H_2} = 1.76$ Å^3 (delays C and c) and 1.75 Å^3 (delays D and d), which were close to the value of 1.74 Å^3 [27]. Due to the intensity fluctuation of the aligning pulses and the vibration of the delay line in the measurements, the measured alignment signals inevitably had slight fluctuation and thus the retrieved $\Delta\alpha_{C_2H_2}$ at different delays showed little difference. Figure 3 shows the measured signals and the calculated signals of C_2H_2 for $\Delta\alpha_{C_2H_2} = 1.80$ Å^3, 1.76 Å^3, and 1.70 Å^3 around delays c and d. The observable distinguishability indicated that the molecular alignment signals of C_2H_2 are polarizability anisotropy sensitive and the error of $\Delta\alpha_{C_2H_2}$ should be around ± 0.06 Å^3.

Moreover, we tried to investigate optical nonlinearity of O_2 and C_2H_2. It was reported that the homodyne and heterodyne signals could be used to estimate the Kerr coefficient n_2 of air molecules [28]. Quite similarly, the total response at delay A (a) in Fig. 2 included the contributions of molecular alignment and optical Kerr effect. This provides us the opportunity to evaluate the Kerr coefficients of O_2 and C_2H_2 via quantitatively analyzing the combined contributions of molecular alignment and optical Kerr effect. The initial value of n_2 was properly chosen and then the contributions of optical Kerr effect ($\delta n_{OK} = n_2 I$) and molecular alignment [$\delta n_{MA} = 2\pi(\rho_0\Delta\alpha/n_0)(\langle\langle\cos^2\theta\rangle\rangle - 1/3)$] were quantitatively calculated. Therefore, we could obtain the total response by adding δn_{OK} and δn_{MA} together and then make a comparison between the total response and the measured signal at delay A (a). In Fig. 4, it indicated that the total responses fitted the measured signals best when the Kerr coefficients of O_2 and C_2H_2 were $n_{2O_2} = 3.05 \times 10^{-19}$ cm^2/W and $n_{2C_2H_2} = 1.89 \times 10^{-18}$ cm^2/W, which were close to the values of $n_{2O_2} = 3.15 \times 10^{-19}$ cm^2/W and $n_{2C_2H_2} = 2.0 \times 10^{-18}$ cm^2/W [29],

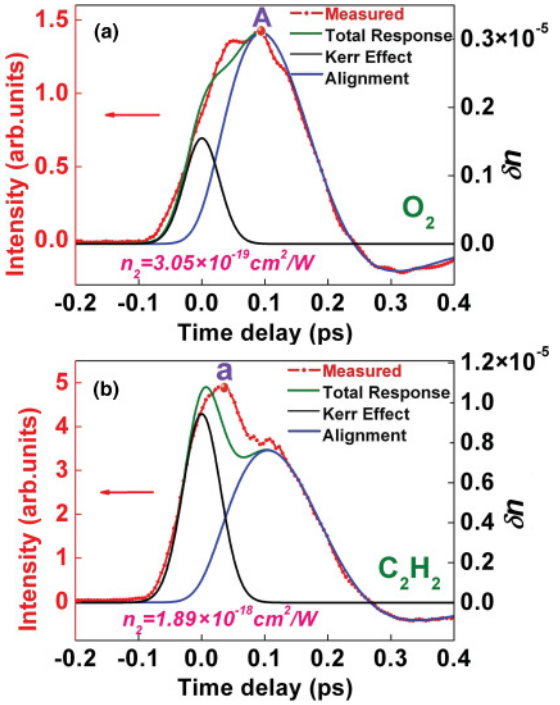

FIG. 4. (Color online) (a), (b) Measured alignment signals (red dot-dash line), the contributions of optical Kerr effect (black solid line), molecular alignment (blue solid line), and the total response (olive solid line) at delays A and a of O_2 and C_2H_2, respectively.

and confirmed the validity of the τ-scan technique in characterizing the optical nonlinearity of gaseous molecules.

IV. CONCLUSION

In conclusion, we have experimentally demonstrated that the polarizability anisotropy of acetylene molecule could be obtained by the τ-scan measurements of spatial focusing and defocusing induced by periodic molecular alignment. The τ-scan technique was also used to measure the Kerr coefficients of oxygen and acetylene by making a comparison between the measured signals around the zero delay and the combined contributions of molecular alignment and optical Kerr effect. This method is also applicable to other molecules, providing a simple and reliable method to investigate the chemical and physical properties of molecules.

ACKNOWLEDGMENTS

This work was partly supported by National Natural Science Fund (Grants No. 10990101 and No. 11004061), National Key Project for Basic Research (Grant No. 2011CB808105), and International Science and Technology Cooperation Program of China (Grant No. 2010DFA04410).

[1] J. A. Fagan, V. Bajpai, B. J. Bauer, and E. K. Hobbie, Appl. Phys. Lett. **91**, 213105 (2007).
[2] R. Ramprasad and N. Shi, Appl. Phys. Lett. **88**, 222903 (2006).
[3] R. I. Keir, D. W. Lamb, G. L. D. Ritchie, and J. N. Watson, Chem. Phys. Lett. **279**, 22 (1997).
[4] T. C. English and K. B. Macadam, Phys. Rev. Lett. **24**, 555 (1970).

[5] Y. Chen and T. Oka, J. Chem. Phys. **88**, 5282 (1988).
[6] S. Minemoto, H. Tanji, and H. Sakai, J. Chem. Phys. **119**, 7737 (2003).
[7] R. Velotta, N. Hay, M. B. Mason, M. Castillejo, and J. P. Marangos, Phys. Rev. Lett. **87**, 183901 (2001).
[8] T. Kanai, S. Minemoto, and H. Sakai, Nature (London) **435**, 470 (2005).
[9] J. J. Larsen, K. Hald, N. Bjerre, H. Stapelfeldt, and T. Seideman, Phys. Rev. Lett. **85**, 2470 (2000).
[10] J. Itatani, J. Levesque, D. Zeidler, Hiromichi Niikura, H. Pépin, J. C. Kieffer, P. B. Corkum, and D. M. Villeneuve, Nature (London) **432**, 867 (2004).
[11] H. Cai, J. Wu, A. Couairon, and H. Zeng, Opt. Lett. **34**, 827 (2009).
[12] J. Wu, H. Cai, A. Couairon, and H. Zeng, Phys. Rev. A **80**, 013828 (2009).
[13] J. Wu, H. Cai, A. Couairon, and H. Zeng, Phys. Rev. A **79**, 063812 (2009).
[14] Y. Feng, H. Pan, J. Liu, C. Chen, J. Wu, and H. Zeng, Opt. Express **19**, 2852 (2011).
[15] H. Cai, J. Wu, H. Li, X. Bai, and H. Zeng, Opt. Express. **17**, 21060 (2009).
[16] X. Yan, Z. Liu, X. Zhang, W. Zang, and J. Tian, Opt. Express **18**, 10270 (2010).
[17] H. Stapelfeldt and T. Seideman, Rev. Mod. Phys. **75**, 543 (2003).
[18] A. Couairon and A. Mysyrowicz, Phys. Rep. **441**, 47 (2007).
[19] V. Renard, O. Faucher, and B. Lavorel, Opt. Lett. **30**, 70 (2005).
[20] J. Wu, H. Cai, Y. Tong, and H. Zeng, Opt. Express **17**, 16300 (2009).
[21] V. Loriot, E. Hertz, A. Rouzée, B. Sinardet, B. Lavorel, and O. Faucher, Opt. Lett. **31**, 2897 (2006).
[22] V. Renard, M. Renard, S. Guerin, Y. T. Pashayan, B. Lavorel, O. Faucher, and H. R. Jauslin, Phys. Rev. Lett. **90**, 153601 (2003).
[23] J. Ortigoso, M. Rodríguez, M. Gupta, and B. Friedrich, J. Chem. Phys. **110**, 3870 (1999).
[24] J. Liu, Y. Feng, H. Li, P. Lu, H. Pan, J. Wu, and H. Zeng, Opt. Express. **19**, 40 (2011).
[25] H. Li, J. Liu, Y. Feng, C. Chen, H. Pan, J. Wu, and H. Zeng, Appl. Phys. Lett. **99**, 011108 (2011).
[26] K. J. Miller, J. Am. Chem. Soc. **112**, 8533 (1990).
[27] A. Rizzo and N. Rahman, Laser Phys. **9**, 416 (1999).
[28] V. Loriot, E. Hertz, O. Faucher, and B. Lavorel, Opt. Express **17**, 13429 (2009).
[29] J. W. Hahn and E. S. Lee, J. Opt. Soc. Am. B **12**, 1021 (1995).